Published in final edited form as:
Science. 2012 February 10; 335(6069): 712–716. doi:10.1126/science.1213979.

Structure and Allostery of the PKA RIIβ Tetrameric Holoenzyme

Ping Zhang[1], **Eric V. Smith-Nguyen**[2], **Malik M. Keshwani**[1,3], **Michael S. Deal**[2], **Alexandr P. Kornev**[2,3], and **Susan S. Taylor**[1,2,3,*]

[1]Howard Hughes Medical Institute, University of California, San Diego, La Jolla, CA 92093–0654, USA

[2]Department of Chemistry and Biochemistry, University of California, San Diego, La Jolla, CA 92093–0654, USA

[3]Department of Pharmacology, University of California, San Diego, La Jolla, CA 92093–0654, USA

Abstract

In its physiological state, cyclic adenosine monophosphate (cAMP)–dependent protein kinase (PKA) is a tetramer that contains a regulatory (R) subunit dimer and two catalytic (C) subunits. We describe here the 2.3 angstrom structure of full-length tetrameric $RII\beta_2:C_2$ holoenzyme. This structure showing a dimer of dimers provides a mechanistic understanding of allosteric activation by cAMP. The heterodimers are anchored together by an interface created by the β4–β5 loop in the RIIβ subunit, which docks onto the carboxyl-terminal tail of the adjacent C subunit, thereby forcing the C subunit into a fully closed conformation in the absence of nucleotide. Diffusion of magnesium adenosine triphosphate (ATP) into these crystals trapped not ATP, but the reaction products, adenosine diphosphate and the phosphorylated RIIβ subunit. This complex has implications for the dissociation-reassociation cycling of PKA. The quaternary structure of the RIIβ tetramer differs appreciably from our model of the RIα tetramer, confirming the small-angle x-ray scattering prediction that the structures of each PKA tetramer are different.

Cyclic adenosine monophosphate (cAMP)–dependent protein kinase (PKA), a ubiquitous serine/threonine protein kinase, exists in mammalian cells as an inactive tetrameric holoenzyme composed of a regulatory (R) subunit dimer and two catalytic (C) subunits. cAMP binding to the R subunits releases the active C subunits, allowing them to phosphorylate specific substrate proteins. The two classes of R subunit, RI and RII, each have α and β isoforms, and these functionally nonredundant isoforms are a primary mechanism for achieving specificity in PKA signaling (1). Deletion of RIα, for example, is embryonically lethal (2), whereas RIIβ knockout mice have a lean phenotype and are not susceptible to diet-induced insulin resistance (3, 4). Depletion of RIIβ reverses the obesity

*To whom correspondence should be addressed. staylor@ucsd.edu.

Supporting Online Material
www.sciencemag.org/cgi/content/full/335/6069/712/DC1
Materials and Methods
Figs. S1 to S7
Tables S1 and S2
References (*39*–*42*)

syndrome of agouti mice (5). RIIβ is the predominant isoform in brain and adipose tissue (2, 6). RII subunits are typically anchored to membrane proteins through high-affinity binding to adenosine kinase–anchoring proteins (AKAPs).

The crystal structure of the C subunit revealed the conserved kinase core shared by all members of the protein kinase superfamily (7, 8). It is bilobal with a large, helical C lobe (Fig. 1A) that facilitates substrate recognition and provides the catalytic machinery for phosphoryl transfer and a smaller, more dynamic beta-rich N lobe that is associated mostly with adenosine triphosphate (ATP) binding (7, 9, 10). The C-terminal tail (C tail), a conserved feature of kinases belonging to the AGC subfamily, serves as a cis-regulatory element that wraps around both lobes and primes the C subunit for catalysis (11).

Each R subunit (Fig. 1A) contains an N-terminal dimerization/docking (D/D) domain, followed by a flexible linker containing an inhibitor site (IS) that docks to the active-site cleft of the C subunit in the holoenzyme. At the C terminus are two tandem highly conserved cyclic nucleotide-binding domains (CNB-A and CNB-B) (12). PKA is anchored to specific sites in the cell by binding of an AKAP amphipathic helix to the D/D domain (13, 14). RII ISs have a Ser at their phosphorylation site (P site) and are both substrates and inhibitors, whereas RI subunits with Gly or Ala at their P site are inhibitors and pseudosubstrates. Phosphorylation of the P-site Ser in RII slows the rate of association with C subunit (15, 16), and formation of holoenzyme in cells is influenced substantially depending on whether the P-site residue is a substrate or a pseudosubstrate (12, 17). In contrast to RII subunits, forming a high-affinity type I holoenzyme with RI subunits requires Mg_2ATP (18).

Complexes of R and C subunits, first described with truncated monomeric R subunits, showed for the first time how the C subunit was inhibited by R and how the complex was activated by cAMP (19–22). These RIα, RIIα, and RIIβ heterodimeric complexes also showed that the R subunits undergo a dramatic conformational change as they release cAMP and bind to C subunit. However, in the absence of cAMP, PKA in cells exists as a tetramer, and only a full-length tetrameric holoenzyme structure will explain how PKA is assembled in its physiological state and how it acquires its allosteric properties. A model of the $(RIα)_2$:C_2 holoenzyme was proposed recently (23), but so far there is no full-length tetrameric structure of PKA. Furthermore, although different PKA holoenzyme isoforms have similar domain organizations, each holoenzyme, based on small-angle x-ray scattering (SAXS), has a different quaternary structure (24, 25); perhaps most notable is the difference between RIIα and RIIβ holoenzymes (24). SAXS showed that both RII homodimers are elongated; however, RIIβ holoenzyme becomes compact, whereas RIIα holoenzyme remains extended. To understand the structural and functional nonredundancy of the PKA isoforms requires structures of tetrameric holoenzymes.

To crystallize a tetrameric $RIIβ_2$:C_2 holoenzyme, we generated wild-type RIIβ(1–416), and, in an effort to stabilize the holoenzyme, we also expressed and purified two mutants that abolished high-affinity binding of cAMP in CNB-A [RIIβ (R230K)] and CNB-B [RIIβ(R359K)], respectively. Only the RIIβ(R230K) holoenyme produced well-diffracting crystals. The crystal structure of the tetrameric $RIIβ(R230K)_2$:C_2 holoenzyme (labeled as

RIIβ*$_2$:C$_2$) was solved at 2.3 Å (Fig. 1, fig. S1, and table S1). Although residues 1 to 103, 122 to 129, and 394 to 416 of RIIβ and residues 1 to 13 of C are missing in the electron density, we validated by using gel electrophoresis that the full-length RIIβ$_2$:C$_2$ complex is in the protein crystal. The absence of density for the N-terminal D/D domain and the following linker is likely related to the flexible nature of this region.

The structure confirms the SAXS predictions (24) that the highly extended RIIβ dimer folded up into a compact holoenzyme (fig. S2). The compact, doughnut-shaped tetramer contains two R:C heterodimers (labeled RC and R′C′) with a rotational twofold symmetry through the central cavity (Fig. 1, B and C). This structure also reveals the dramatic changes that take place in the RIIβ subunit as it releases cAMP and binds to C subunit (Fig. 1D). In the cAMP-bound state, two hydrophobic capping residues (Arg^{381R} for CNB-A and Tyr^{397R} for CNB-B) are bound to the adenine rings of cAMP (26, 27). These two residues move away from the cAMP binding sites in the holoenzyme (38 Å for Arg^{381R}) and are kept in this distal location by a holoenzyme-specific salt bridge between Arg^{392R} and Glu^{282R} (Fig. 1D). This salt bridge is important for allosteric activation (20, 22) and is conserved in all R-subunit isoforms (12).

The C subunits are well separated, whereas each R subunit contacts the neighboring R:C heterodimers by using the highly conserved but isoform-specific β4–β5 loop in the CNB-A domain (fig. S3). This loop is exposed to solvent in the free cAMP-bound R subunit (Fig. 1D) and also in the heterodimer (20, 22); however, in the tetramer it reaches over to the opposite dimer and creates an extensive interface. The area of each interface between the two heterodimers, which are strictly twofold rotational symmetry related, is ~500 Å^2. The major site of contact is to the C-terminal tail of the opposite C subunit, specifically the active-site tether (AST, residues 320 to 339) segment. The C tail (residues 301 to 350 in PKA) is a highly conserved feature of all AGC kinases (11). Residues 301 to 318, referred to as the C-lobe tether, are anchored firmly to the C lobe, whereas residues 336 to 350, referred to as the N-lobe tether, are anchored through a hydrophobic motif to the N lobe. The intervening AST segment, typically disordered in the absence of nucleotide, becomes an integral part of the ATP binding site when nucleotide is bound. A conserved Phe-Asp-Asp-Tyr (FDDY) motif (residues 327 to 330) in this region, in particular Phe^{327C} and Tyr^{330C}, are part of the hydrophobic pocket that anchors the adenine and ribose rings of ATP. When either residue is replaced with Ala, enzymatic activity is lost and affinity for ATP is reduced (28, 29). In the holoenzyme, the β4–β5 loop docks to the back of the FDDY motif, pushing it and the entire N lobe into a fully closed conformation even though the nucleotide is absent. The β4–β5 loop also interacts with a portion of the R-subunit N linker from the opposite heterodimer. The details of these interactions are described in fig. S3.

Ordering of the C tail and the N lobe by the β4–β5 loop into a closed conformation independent of ATP is one of the most striking features of the RIIβ tetrameric holoenzyme and distinguishes it from the heterodimer and from all previous structures of the C subunit, which are only in a closed conformation when ATP and two magnesium ions are bound (Fig. 2A). In this structure, Ser^{53C} at the tip of the Gly-rich loop interacts with the backbone carbonyl of the P-site Ser^{112R}, and this is a hallmark of the closed conformation. Ser^{112R} also forms hydrogen bonds with catalytic loop residues Asp^{166C} and Lys^{168C} (Fig. 2A). In

the RIα heterodimer, the C subunit is also in a closed conformation that requires Mg_2ATP, whereas in the RIIα heterodimer, where high-affinity binding does not require Mg_2ATP (18), the C subunit is in an open conformation with an empty ATP binding pocket and a disordered C tail (Fig. 2B) (20, 22). Comparing temperature factors (B factor) of C subunits in different R:C complexes reveals regions of relative order and disorder (Fig. 2B and table S2). The nucleotide-bound RIα(91–379):C heterodimer is in a fully closed conformation and has low B-factors both in the N and C lobe (Fig. 2B and table S2). In contrast, the nucleotide-free RIIα(90–400):C dimer has high B factors in the N lobe, and the C tail is partially disordered, consistent with its open conformation (Fig. 2B). The apo nucleotide-free tetrameric holoenzyme, similar to the nucleotide-bound RIα complex, has low B factors in both lobes, which reflects its closed conformation and ordered C tail (Fig. 2B).

The allosteric properties of the RIIβ holoenzyme are also different from the RIIβ heterodimer and from the other three PKA isoforms. The activation constant (K_a) for activation of the RIIβ tetramer by cAMP is 584 nM, and this is significantly higher than the K_a for other holoenzymes [101 nM for RIα (30), 29 nM for RIβ (31), and 137 nM for RIIα (Fig. 4A)]. It is also higher than the K_a of 65nM for RIIβ heterodimer (Fig. 3). The increased K_a for the RIIβ tetrameric holoenzyme can be explained by the extensive interfaces between the two heterodimers, where the phosphate-binding cassette (PBC) docking site for cAMP in CNB-A is juxtapositioned directly against the ATP binding site in N lobe of the C subunit in the opposite heterodimer (Fig. 3B). The Hill coefficient for the RIIβ tetramer is 1.7, in contrast to 0.65 for the heterodimers, which indicates that allostery is unique to the tetramer. The considerable cross-talk between the two CNB domains and the between the two heterodimers is also reflected by several mutations. When the CNB-B domain is deleted entirely, for example, the K_a for activation is 60 nM and the Hill coefficient is reduced to 1.2, indicating that there is still substantial allosteric cross-talk between the two CNB-A domains (31, 32) (Fig. 3C). When the cAMP binding site in the CNB-A domain is deleted, the K_a for activation is very high, 13 μM, confirming that cAMP binding to CNB-A is essential for activation. However, when the B domain is mutated, the enzyme still has a similar K_a for activation (490 nM), but all cooperativity is lost. The molecular basis for this complex allostery could simply not be appreciated in the absence of the holoenzyme structure.

Given that the ATP binding chamber in the C subunit is perfectly formed and locked into a closed conformation, we hypothesized that ATP could diffuse into this pocket without breaking the crystal lattice. We thus soaked the apo crystals with MgATP (materials and methods). The resulting crystals, solved to a resolution of 3.1 Å (table S1), showed that nucleotide had diffused into the active site. However, instead of finding ATP, we found the reaction products, Mg_2ADP and the phosphorylated RIIβ subunit (Fig. 4 and fig. S5). This is the first time that we have trapped both reaction products in the active-site cleft, and such a complex has also not been observed for other protein kinases. Even trapping a transition state complex has been challenging, and PKA is one of the few examples where this has been possible (33). The overall $RII\beta^{P}{}_2{:}C_2{:}(Mg_2ADP)_2$ structure closely resembles the apo $RII\beta^{*}{}_2{:}C_2$ structure (fig. S5) with a Cα root mean square deviation (RMSD) of 0.67 Å. The C subunit still remains in a closed conformation and still has low B factors in both the C and

N lobe (table S2). The B factors in the phosphorylated inhibitor site of RIIβ are also low. There is an ~5 Å shift of the tip residue Ser^{53C} in the Gly-rich loop from its position in the apo structure, which is sufficient to break the hydrogen bond between the Ser^{53C} and Ser^{112R} (Fig. 2A and fig. S5). Thus, the $RII\beta^{P}_2$:C_2:$(Mg_2ADP)_2$ tetramer contains a perfectly formed stable reaction chamber that allows for catalysis, but the reaction products were trapped. We hypothesize that this complex may be a physiologically relevant state for the RIIβ holoenzyme.

Typically the $RII\beta_2$:C_2 holoenzyme is colocalized through AKAPs with protein phosphatases (PPs) (34). For example, calcineurin, a calcium-activated phosphatase, and PKA RII holoenzymes are colocalized at the C terminus of AKAP79/150 (34). Because the RII inhibitor sites are excellent substrates for calcineurin, it has been assumed that the RIIβ subunit is dephosphorylated by calcineurin to facilitate its reassociation with C subunits (15, 16). However, a recent report suggests that the RII subunits in cardiac myocytes are mostly phosphorylated in the absence of forskolin (35). Although this observation needs to be further validated, our structure suggests that in cells the inactive $RII\beta_2$:C_2 holoenzyme, once formed, may be primed to have its R subunits autophosphorylated (Fig. 4C) given the high availability of cytoplasmic MgATP. This presents the following scenario. Cooperative cAMP activation leads to dissociation of the C subunits from the $RII\beta^{P}$ homodimer. Nearby phosphatases like calcineurin, localized in close proximity to the RII holoenzyme (34, 36), can then modulate PKA activity by dephosphorylating the $RII\beta^{P}$ subunit when calcium levels are elevated, thereby facilitating the regeneration of inactive $RII\beta_2$:C_2 holoenzyme (15, 16). This apo $RII\beta_2$:C_2 holoenzyme can then get autophosphorylated with cytoplasmic MgATP yet stay in an inactive form (Fig. 4C) until cAMP levels are elevated again.

Anchoring of RII holoenzymes near membranes is mediated by the D/D domain binding to AKAPs, and, from the position of the traced N linker of the two RIIβ chains (fig. S6) and the available space in crystal packing, the position of the missing D/D domain can be predicted. In our RIIβ structure, the first 13 residues of the C subunit are disordered, whereas in the free C subunit the myristyl group is folded into a hydrophobic pocket in the C lobe of the C subunit (37). Fluorescence anisotropy studies showed that binding of the RIIβ subunit causes the myristylated N tail to become more flexible and dynamic, and, in contrast to free C and the RIα tetramer, the RII holoenzyme interacts with membrane vesicles (38). When the RIIβ holoenzyme is targeted by AKAPs to membrane proteins, the exposed myristyl groups will likely be on the same surface as the AKAP, which provides an opportunity for multivalent membrane anchoring. The holoenzyme targeted to membranes also has the potential to interact with other signaling proteins, such as adenylylate cyclases (ACs), heterotrimeric guanine nucleotide–binding (G) proteins, G protein–coupled receptors (GPCRs), and phosphodiesterases (PDEs) in addition to AKAPs, and thus could contribute to the assembly of larger macromolecular complexes. These interactions would create enormous opportunities for synergy that now need to be considered more rigorously.

A comparison of our model of the RIα tetrameric holoenzyme (23) with the RIIβ holoenzyme (Fig. 5 and fig. S7) shows how isoform-specific quaternary structures can be created even though the tertiary structures of the heterodimers are remarkably similar for RIα, RIIα (20, 22), and RIIβ. By forming a dimer of dimers, a twofold axis of symmetry is

created in the tetrameric holoenzyme; however, the specific interface between the dimers is different for each R-subunit isoform. In each case, however, the β4–β5 loop in the R subunit appears to serves a specificity determinant for docking between the two heterodimers. By comparing the RIIβ tetramer with a model of the RIα holoenzyme, we see how distinct quaternary architectures can be created. It is only by comparing the full-length holoenzymes that we can appreciate that the functional nonredundancy of the PKA isoforms is also reflected in the structural nonredundancy of these isoforms. Correlating these structural differences with functional consequences will be our next challenge.

Supplementary Material

Refer to Web version on PubMed Central for supplementary material.

Acknowledgments

We thank members of the Taylor laboratory for helpful discussions and the Advanced Light Source (beam line 8.2.2) staff of Lawrence Berkeley National Laboratory for beam access and help with data collection. This work was supported by NIH grant GM34921 (S.S.T.). Coordinates and structure factors have been deposited in the Protein Data Bank (PDB) with accession numbers 3TNP and 3TNQ.

References and Notes

1. Amieux PS, et al. J Biol Chem. 2002; 277:27294. [PubMed: 12004056]
2. Amieux PS, et al. J Biol Chem. 1997; 272:3993. [PubMed: 9020105]
3. Cummings DE, et al. Nature. 1996; 382:622. [PubMed: 8757131]
4. Schreyer SA, Cummings DE, McKnight GS, LeBoeuf RC. Diabetes. 2001; 50:2555. [PubMed: 11679434]
5. Czyzyk TA, Sikorski MA, Yang L, McKnight GS. Proc Natl Acad Sci USA. 2008; 105:276. [PubMed: 18172198]
6. McConnachie G, Langeberg LK, Scott JD. Trends Mol Med. 2006; 12:317. [PubMed: 16809066]
7. Knighton DR, et al. Science. 1991; 253:407. [PubMed: 1862342]
8. Manning G, Whyte DB, Martinez R, Hunter T, Sudarsanam S. Science. 2002; 298:1912. [PubMed: 12471243]
9. Cheng X, Phelps C, Taylor SS. J Biol Chem. 2001; 276:4102. [PubMed: 11110787]
10. Johnson DA, Akamine P, Radzio-Andzelm E, Madhusudan M, Taylor SS. Chem Rev. 2001; 101:2243. [PubMed: 11749372]
11. Kannan N, Haste N, Taylor SS, Neuwald AF. Proc Natl Acad Sci USA. 2007; 104:1272. [PubMed: 17227859]
12. Canaves JM, Taylor SS. J Mol Evol. 2002; 54:17. [PubMed: 11734894]
13. Kinderman FS, et al. Mol Cell. 2006; 24:397. [PubMed: 17081990]
14. Newlon MG, et al. EMBO J. 2001; 20:1651. [PubMed: 11285229]
15. Diskar M, Zenn HM, Kaupisch A, Prinz A, Herberg FW. Cell Signal. 2007; 19:2024. [PubMed: 17614255]
16. Rangel-Aldao R, Rosen OM. J Biol Chem. 1976; 251:3375. [PubMed: 179996]
17. Martin BR, Deerinck TJ, Ellisman MH, Taylor SS, Tsien RY. Chem Biol. 2007; 14:1031. [PubMed: 17884635]
18. Herberg FW, Taylor SS. Biochemistry. 1993; 32:14015. [PubMed: 8268180]
19. Brown SH, Wu J, Kim C, Alberto K, Taylor SS. J Mol Biol. 2009; 393:1070. [PubMed: 19748511]
20. Kim C, Cheng CY, Saldanha SA, Taylor SS. Cell. 2007; 130:1032. [PubMed: 17889648]
21. Kim C, Xuong NH, Taylor SS. Science. 2005; 307:690. [PubMed: 15692043]
22. Wu J, Brown SHJ, von Daake S, Taylor SS. Science. 2007; 318:274. [PubMed: 17932298]

23. Boettcher AJ, et al. Structure. 2011; 19:265. [PubMed: 21300294]
24. Vigil D, Blumenthal DK, Taylor SS, Trewhella J. J Mol Biol. 2006; 357:880. [PubMed: 16460759]
25. Heller WT, et al. J Biol Chem. 2004; 279:19084. [PubMed: 14985329]
26. Berman HM, et al. Proc Natl Acad Sci USA. 2005; 102:45. [PubMed: 15618393]
27. Diller TC, Xuong NH, Taylor SS. Protein Expr Purif. 2000; 20:357. [PubMed: 11087674]
28. Batkin M, Schvartz I, Shaltiel S. Biochemistry. 2000; 39:5366. [PubMed: 10820007]
29. Yang J, et al. J Biol Chem. 2009; 284:6241. [PubMed: 19122195]
30. Herberg FW, Taylor SS, Dostmann WR. Biochemistry. 1996; 35:2934. [PubMed: 8608131]
31. Cadd GG, Uhler MD, McKnight GS. J Biol Chem. 1990; 265:19502. [PubMed: 2174040]
32. Zawadzki KM, Taylor SS. J Biol Chem. 2004; 279:7029. [PubMed: 14625280]
33. Madhusudan P, Akamine NH, Xuong SS, Taylor. Nat Struct Biol. 2002; 9:273. [PubMed: 11896404]
34. Oliveria SF, Dell'Acqua ML, Sather WA. Neuron. 2007; 55:261. [PubMed: 17640527]
35. Manni S, Mauban JH, Ward CW, Bond M. J Biol Chem. 2008; 283:24145. [PubMed: 18550536]
36. Hall DD, et al. Biochemistry. 2007; 46:1635. [PubMed: 17279627]
37. Zheng J, et al. Protein Sci. 1993; 2:1559. [PubMed: 8251932]
38. Gangal M, et al. Proc Natl Acad Sci USA. 1999; 96:12394. [PubMed: 10535933]

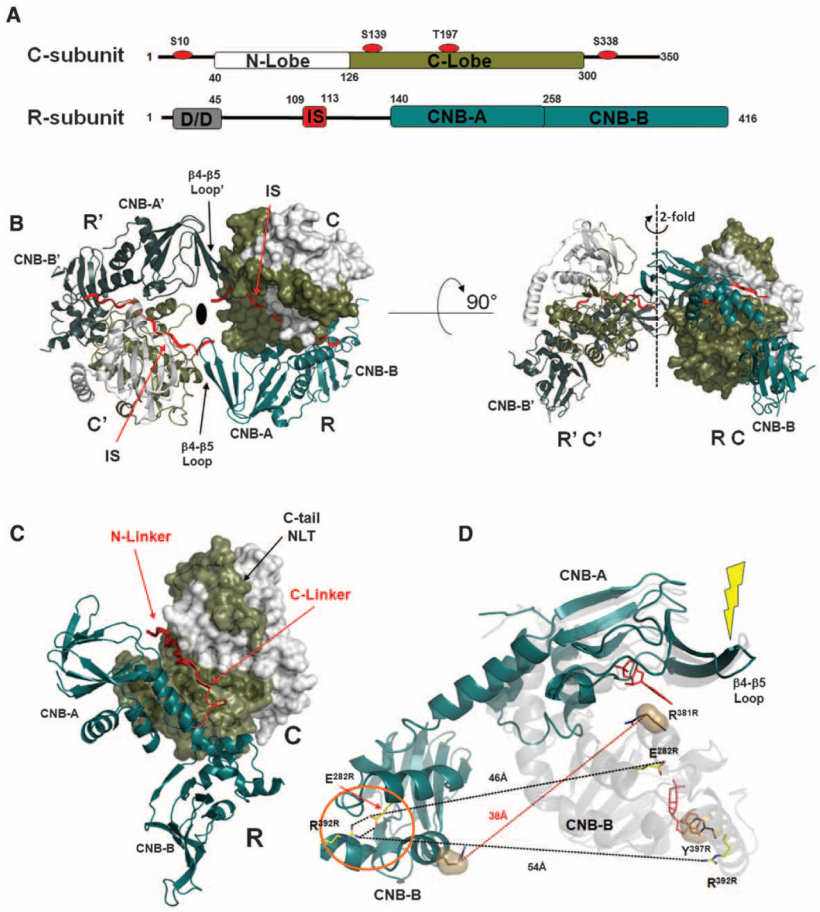

Fig. 1.

Overall view of the RIIβ*$_2$:C$_2$ tetrameric holoenzyme. (**A**) Domain organization and color coding of the R and C subunits. The four red spheres indicate the phosphorylation sites in C subunit. (**B**) Structure of the RIIβ*$_2$:C$_2$ tetrameric holoenzyme. The N lobe of the C subunit is white; the C lobe and C tail are tan. The N-linker segment of the R subunit that contains the IS and docks to the active-site cleft of the C subunit is shown as a red ribbon. One heterodimer is labeled as RC, and its twofold symmetry mate is labeled as R′C′. The twofold axis position is shown as a black oval (left) and dotted line (right). (**C**) One RIIβ:C heterodimeric holoenzyme structure in the RIIβ*$_2$:C$_2$ tetrameric holoenzyme. (**D**) RIIβ undergoes dramatic conformational changes upon binding to the C subunit. RIIβ bound to the C subunit is shown on the left and bound to cAMP shown on the right (PDB ID code 1CX4, in black). The salt bridge Glu^{282R}-Arg^{392R} formed upon binding to the C subunit is shown in an orange circle.

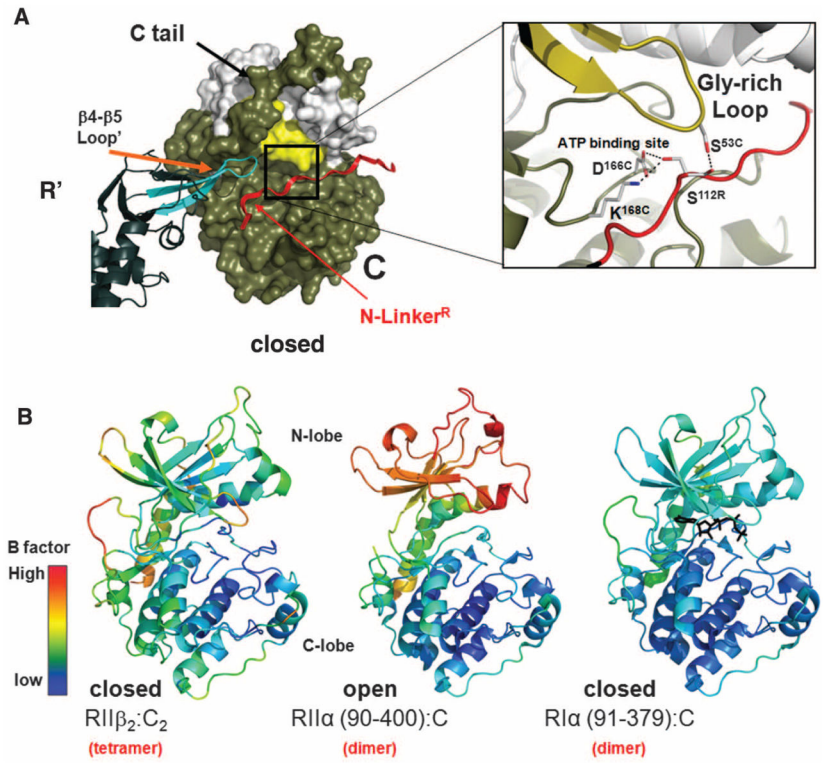

Fig. 2.

C subunit is in a closed conformation. (**A**) The active site of the C subunit in the RIIβ*$_2$:C$_2$ tetrameric holoenzyme is fully closed in the absence of ATP. S, Ser; K, Lys. (**B**) The conformation and B factors analysis of the C subunit in three holoenzyme structures. The left bottom is the scale bar for B factors.

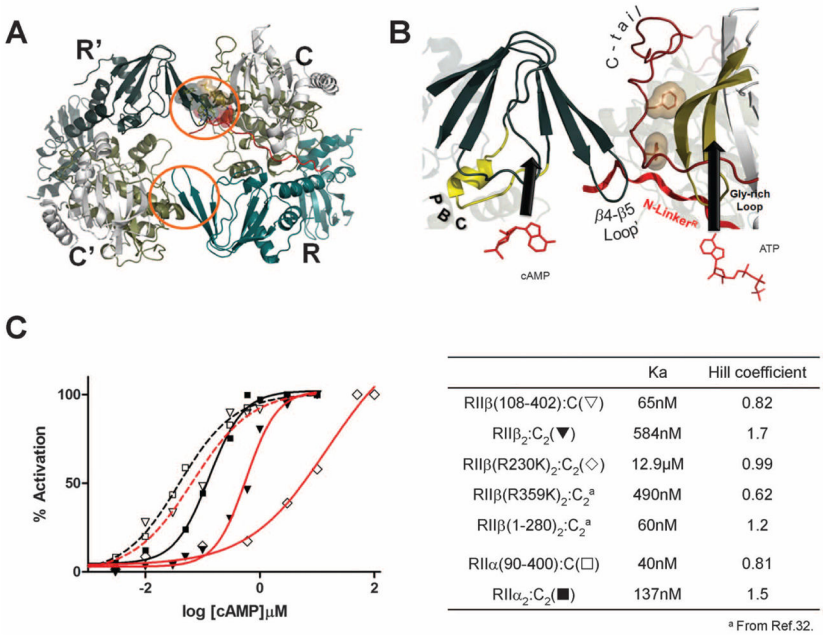

	Ka	Hill coefficient
RIIβ(108-402):C(▽)	65nM	0.82
$RIIβ_2$:C_2(▼)	584nM	1.7
$RIIβ(R230K)_2$:C_2(◇)	12.9μM	0.99
$RIIβ(R359K)_2$:C_2[a]	490nM	0.62
$RIIβ(1-280)_2$:C_2[a]	60nM	1.2
RIIα(90-400):C(□)	40nM	0.81
$RIIα_2$:C_2(■)	137nM	1.5

[a] From Ref.32.

Fig. 3.

Allosteric cAMP activation mechanism for the RIIβ holoenzyme. (**A**) Overall interactions of the RC and R′C′. The two symmetry-related interfaces are shown in orange circles. (**B**) The binding site for cAMP to CNB-A′ in R′C′ heterodimer (left arrow) is juxtapositioned directly against the ATP binding site (right arrow) in the N lobe of the C subunit in the symmetry-related RC dimer. (**C**) Activation of holoenzymes by cAMP. The K_a values for activation were measured as a function of cAMP. Each holoenzyme is designated as follows: RIIα(90–400):C(□), RIIβ(108–402):C(▽), $RIIα_2$:C_2(□), WT $RIIβ_2$:C2(▼), and $RIIβ*_2$:C_2(◇).

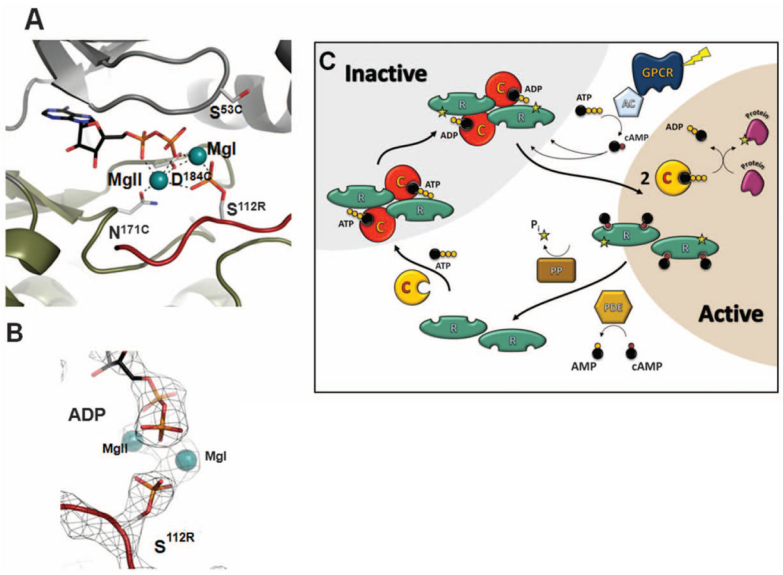

Fig. 4.

RIIβ$^{P}_{2}$:C_2:(Mg_2ADP)$_2$ tetrameric holoenzyme. (**A**) Two Mg^{2+} ions coordinate interactions in the active site of RIIβ$^{P}_{2}$:C_2:(Mg_2ADP)$_2$. MgI coordinates the β phosphate of ADP, the transferred γ phosphate, and residue Asp^{184C} in the DFG loop; whereas MgII coordinates both α and β phosphates of ADP, the transferred γ phosphate, and residues Asp^{184C} and Asn (N)^{171C}. (**B**) Electron density map of ATP hydrolyzed to ADP and γ phosphate transferred to P-site Ser^{112R}. (**C**) Schematic model of auto-phosphorylation of RIIβ in cells.

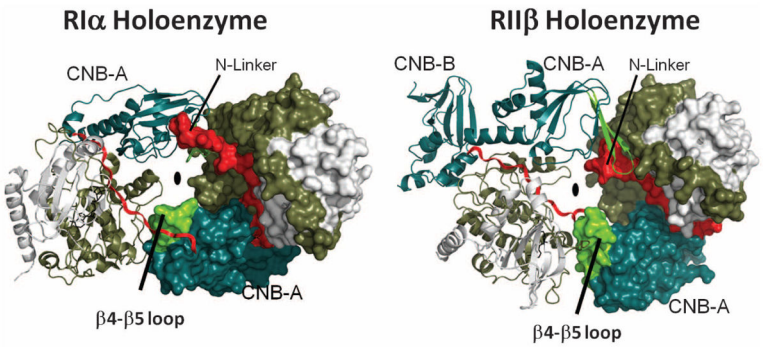

Fig. 5.

Comparison of $RI\alpha_2:C_2$ model (3PVB) and $RII\beta^*_2:C_2$ structure. Although each holoenzyme creates a twofold symmetry, the interface is completely different in the two tetramers. The N-linker is red and β4–β5 loop is green. The axes of symmetry are also indicated by the black ovals.